Thermochimica Acta, 238 (1994) 203–227
Elsevier Science B.V., Amsterdam
SSDI 0040-6031(93)01579-R

The melting of polymers — a three-phase approach

M. Alsleben and C. Schick *
University of Rostock, Department of Physics, Universitätsplatz 3, D-18051 Rostock (Germany)

(Received 3 February 1993; accepted 25 October 1993)

Abstract

Information on the morphology of semi-crystalline polymers can be obtained from their melting behaviour. Due to the lamellae thickness distribution, a very broad melting region is observed. From a comparison of the glass transition intensity and the crystallinity, e.g. from X-ray diffractometry, it is known that there are rigid amorphous regions inside semi-crystalline polymers with no contribution to the glass transition or to the melting. Both the broad melting region and the deviation from the normally used two-phases model often result in incorrect crystallinities and other morphological parameters. Therefore, the analysis of the melting behaviour, taking into account the broad melting region and the rigid amorphous fraction, should result in a better, more detailed description of the morphology. A procedure to do this on the basis of a separation of the measured heat flux into the baseline specific heat capacity and the excess portion is suggested here. Using this procedure, it should be possible to obtain the temperature dependence of the crystalline, rigid amorphous, and liquid amorphous fractions, as well as the lamellae thickness distribution, the thickness of the interfaces of the lamellae, and the specific inner surface of the crystalline fraction.

INTRODUCTION

Polymers, like other substances, can exist in different states (liquid, crystalline, glassy). In some, these states can coexist at the same temperature. Such substances are called semi-crystalline. One aim of the thermal analysis of semi-crystalline materials is to determine the fractions of the different states. To obtain more detailed information on the morphology, it is necessary to combine these with results from other methods, e.g. X-ray diffractometry. Thus, it is possible to obtain information on the dimensions of the structural units, the distributions of these dimensions, the internal surface of the crystalline regions, etc.

A simple way to describe semi-crystalline structures is by using a two-phase model, containing material in the crystalline and amorphous

* Corresponding author.

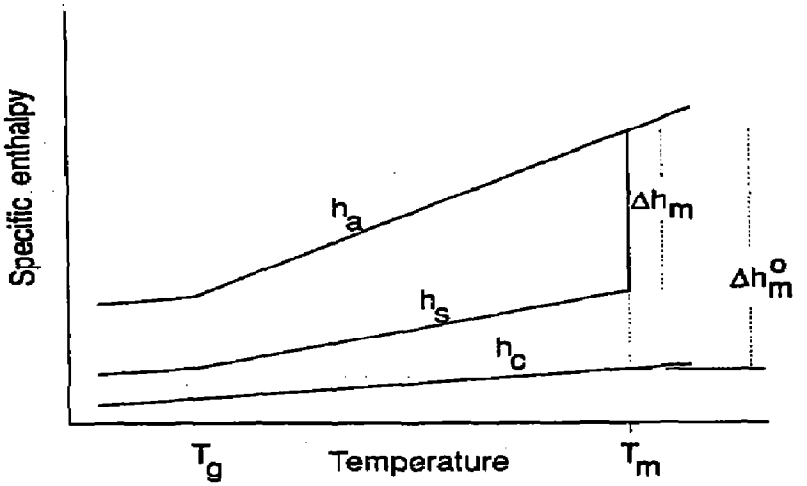

Fig. 1. Simplified specific enthalpy curves of the crystalline (h_c), amorphous (h_a) and semi-crystalline (h_s) states with heating. The slope of the specific enthalpy curves of the amorphous and semi-crystalline states increases at the glass temperature T_g. At the melting temperature T_m, the specific enthalpy of the crystalline material becomes that of the liquid state, with a jump of height Δh_m (semi-crystalline sample) and Δh_m^o (fully crystalline sample), respectively.

states only. In the following we will briefly discuss the thermal behaviour of such a two-phase system.

From the thermal analysis, it is possible to obtain information on the enthalpy and the specific heat capacity. For both, the measured quantity for a semi-crystalline sample (index s) is the superposition of that of the amorphous (index a) and the crystalline (index c) fractions. Simplified curves are shown in Figs. 1 and 2.

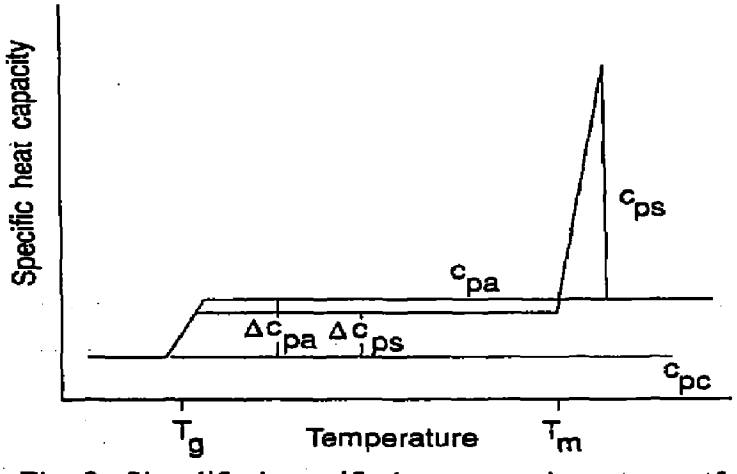

Fig. 2. Simplified specific heat capacity curves of the crystalline (c_{pc}), amorphous (c_{pa}) and semi-crystalline (c_{ps}) states with heating. At the glass temperature T_g, a jump occurs in the specific heat capacity of the liquid (Δc_{pa}) and semi-crystalline (Δc_{ps}) states.

For temperatures below the glass temperature T_g, the specific heat capacity, and therefore the slope of the specific enthalpy curves for the glassy and crystalline states, is practically the same. At T_g, the specific heat capacity increases. In the two-phase model, it is assumed that all the amorphous fraction is in a mobile, liquid amorphous state (index l below) above the glass transition temperature T_g. For a semi-crystalline sample, the height of the jump at T_g (Δc_{ps}) depends on the degree of crystallinity.

At the melting temperature T_m, material in the crystalline state will transform into the liquid amorphous state. The specific enthalpy of the liquid amorphous state will be reached at this temperature by a jump. The difference between the specific enthalpy of the amorphous and the crystalline state Δh_m^0 depends on the temperature (Fig. 1). In semi-crystalline systems, the difference between the specific enthalpy of the amorphous and the semi-crystalline state Δh_m is related to the crystalline fraction and also depends on the temperature [1–3]. Therefore, the crystalline fraction α at a temperature T can be calculated from the specific enthalpy of the crystalline state h_c, the specific enthalpy of the amorphous state h_a, and the specific enthalpy of the semi-crystalline state h_s (see Fig. 1) by

$$\alpha(T) = \frac{h_a(T) - h_s(T)}{h_a(T) - h_c(T)} = \frac{\Delta h_m(T)}{\Delta h_m^0(T)} \tag{1}$$

Various methods to determine this ratio have been described, for example by Gray [1], Richardson [2] and Mathot and Pijpers [3].

For some polymers and other semi-crystalline substances, a glass transition can be observed in the amorphous and in the semi-crystalline state. Because the glass transition in a semi-crystalline sample occurs in the amorphous fraction only, an analysis of the glass transition (see Fig. 2) is another possible way of evaluating the fractions [4, 5]. The step height Δc_{ps} at the glass transition depends on the fraction γ of the mobile amorphous material. The fraction may be calculated by

$$\gamma = \frac{\Delta c_{ps}}{\Delta c_{pa}} \tag{2}$$

where Δc_{pa} is the step height of a fully amorphous sample. Then, in a two-phase model, the remainder of the material $(1 - \gamma)$ should be in the crystalline state.

To prove the applicability of the two-phase model, the crystallinities calculated from the specific melting enthalpy and those from the step height of the specific heat capacity at the glass transition can be compared. If only the crystalline and melt-like amorphous fractions are present, the

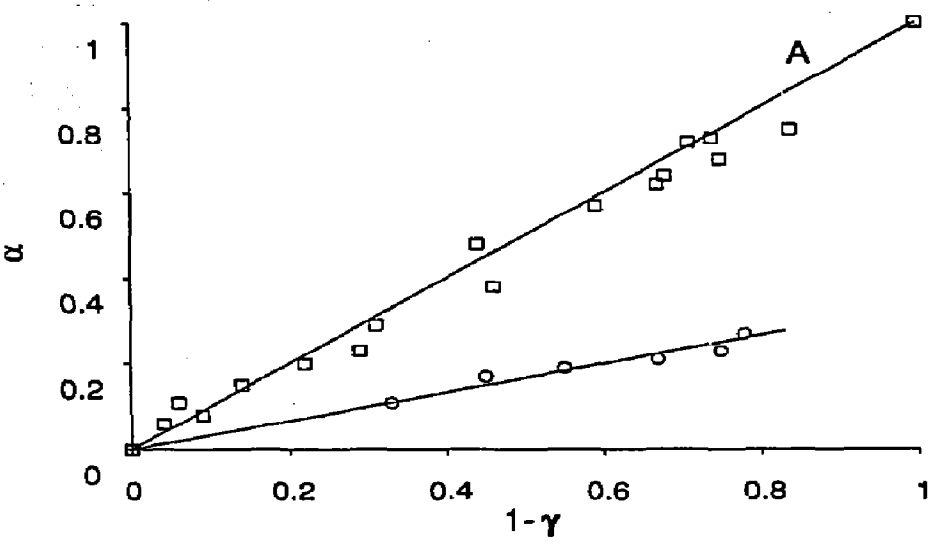

Fig. 3. The relation between the crystallinities determined from the glass transition ($1-\gamma$) and the melting enthalpy (α) for a low molecular mass liquid crystal [6] (□) and a PET sample (○) isothermally crystallized at 390 K. Line A represents the two-phase behaviour.

crystallinities calculated by these two approaches should be the same for one sample. The results of this comparison for a low molecular mass substance [6] and for a polymer are shown in Fig. 3 [7, 8].

For the low molecular mass substance, the crystallinities calculated by these two methods are the same, which means that the two-phase model will describe the behaviour of the low molecular mass substance correctly. In the case of the semi-crystalline polymer, poly(ethylene terephthalate) (PET), there is a significant difference between the crystallinities calculated from the glass transition and from the melting. Wunderlich and coworkers [4, 5] concluded from this that a third fraction occurs in the case of semi-crystalline polymers. This fraction is structurally amorphous but is present in the glassy state, often up to the melting temperature of the lamellae. It does not take part in the glass transition at the normal T_g. Here, it is called the rigid amorphous fraction β. The rigid amorphous fraction may be calculated by

$$\beta = 1 - \gamma - \alpha \tag{3}$$

In the case of PET, the rigid amorphous fraction is in the range of 0.32 up to 0.59 [8, 9]. Therefore, the rigid amorphous fraction should not be neglected in the discussion of the morphology and the melting behaviour. A morphological model for polymers crystallized in the form of lamellae stacks, including the rigid amorphous state, will be described below. This model will then be used to discuss the melting of polymers.

MODEL

Electron microscopic investigations [10, 11] show that some semi-crystalline polymers, such as PE, PET and PP, crystallize in the form of lamellae whose lateral dimensions are much larger than the lamellae thicknesses. It is also apparent from electron microscopic investigations that such lamellae often build up in stacks. Therefore, the normal model of the morphology of polymers crystallizing in the form of lamellae is a one-dimensional two-phase layer stack model [12]. This model is mainly used in the interpretation of SAXS investigations. It consists of alternately ordered crystalline layers of thickness d_c and volume fraction α, and amorphous layers of thickness d_a and the volume fraction $1 - \alpha$. The mean distance between the centres of the crystalline layers is called the long period L.

However, the layer stack model must also include rigid amorphous layers. We assume that these layers are equal to the interfacial layers of the lamellae (Fig. 4).

The one-dimensional layer stack model now includes the crystalline layers (lamellae) with thickness d_c, mobile amorphous layers with thickness d_l and two rigid amorphous interfacial layers with thickness d_i, within one long period L (Fig. 4).

In order to apply this model to the description of the melting behaviour of semi-crystalline polymers, three morphological assumptions have to be made

(i) The sample is completely filled with the stack structures shown in Fig. 4. If a sample is not completely crystallized, which means as completely as possible, larger melt-like amorphous regions must be considered [8, 13].

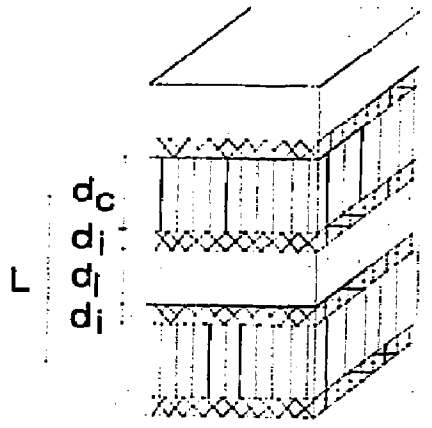

Fig. 4. Stack of lamellae in semi-crystalline polymers: L is the long period; d_c, d_i and d_l, the thicknesses of the crystalline (lamella), rigid amorphous (interfacial), and mobile amorphous (liquid) layers, respectively.

(ii) The lateral layer extension is much larger than their thickness (d_c, d_l, d_i). Thus, the layer thicknesses can be determined from a one-dimensional model (eqn. (4)).
(iii) The layers are homogeneous. The transitions between the layers are relatively sharp. Non-crystalline areas inside the lamella are associated with the interfacial layer.

If these assumptions are fulfilled, the number-averaged mean thicknesses of the layers may be determined from the long period L and the volume fractions α, β, γ by

$$d_c = L\alpha \qquad d_l = L\beta/2 \qquad d_i = L\gamma \tag{4}$$

In the following discussion, the differences between volume and mass fractions are ignored.

Because the specific enthalpy of a sample is the superposition of the enthalpies of the different fractions, it is necessary to include in specific enthalpy diagram (Fig. 1) the specific enthalpy of the rigid amorphous state (Fig. 5). To do this, we consider the cooling of a polymer melt. Down to the crystallization temperature T_c, there is only liquid amorphous material of specific enthalpy h_l, hence the specific enthalpy of the sample h_s is the same as that of the liquid amorphous state. At the crystallization temperature T_c, crystalline lamellae of specific enthalpy h_c are formed. According to the specific enthalpy of the liquid amorphous state, the specific enthalpy h_c is lowered by the specific heat of fusion Δh_c^0. At this temperature, in addition, the interfaces of the lamellae are formed, because of the hindering of the

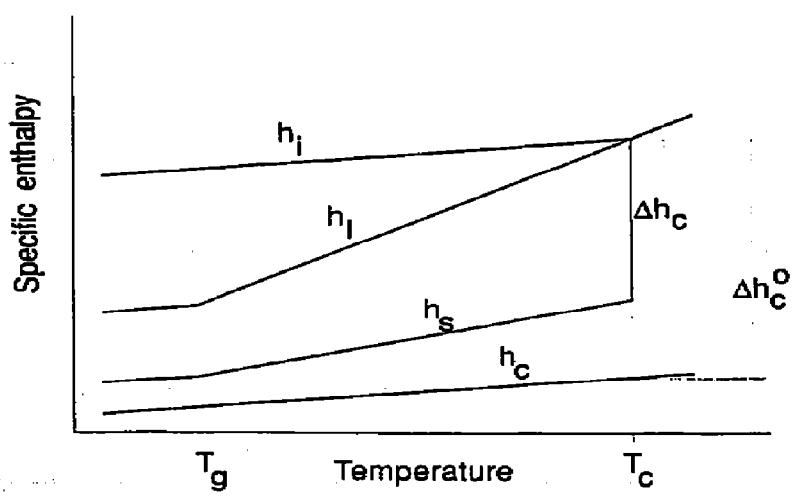

Fig. 5. Simplified specific enthalpy curves of the crystalline (h_c), liquid (h_l), interface (h_i), and semi-crystalline (h_s) states (see Fig. 1): T_c, crystallization temperature, T_g, glass transition temperature, Δh_c^0 specific crystallization enthalpy of the fully crystalline state; Δh_c, specific crystallization enthalpy of the semi-crystalline state.

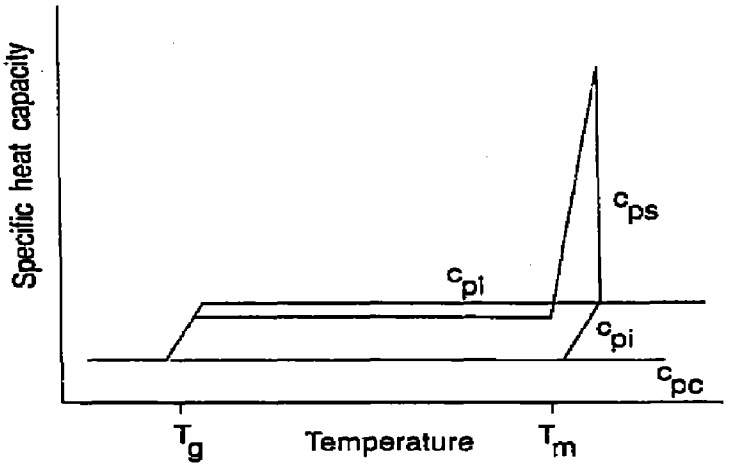

Fig. 6. Simplified specific heat capacity curves of the crystalline (c_{pc}), liquid (c_{pl}), interface (c_{pi}), and semi-crystalline (c_{ps}) states (see Fig. 2).

molecular mobility in the surroundings of the lamellae. So the material in the interfaces becomes rigid (glassy) at the crystallization temperature and therefore the vitrification temperature of the material in the interfaces is the crystallization temperature of the lamellae. This is why the slope of the specific enthalpy curve of the interfaces h_i changes at the crystallization temperature.

The specific enthalpy diagram of the heating process is in principle the same (deviations are discussed below). Up to the melting temperature T_m, the specific enthalpy of the sample is the superposition of the specific enthalpies of the crystalline, rigid amorphous (glassy), and liquid states. At this temperature, the lamellae and, hence, their interfaces will disappear. Thus the specific enthalpy curves of the lamellae (melting) and the interfaces (glass transition) change to those of the liquid material. From this, the specific heat capacity curves of the sample on heating (Fig. 6) are available.

Using the "three-phase" model, described above, it is also possible to obtain information on the fractions, from both the melting behaviour and the glass transition. So it should be possible to combine both to obtain more detailed information on the examined sample.

RESULTS FROM THE GLASS TRANSITION

A major question in the morphological analysis of semi-crystalline polymers is whether assumption (iii) of the model (above) is permissible. For this, the mobile amorphous fraction in particular, as determined from the glass transition (relaxation) intensity (eqn. (2)), is compared with

results obtained by different methods, e.g. DSC, NMR and Raman spectroscopy [8, 9, 14]. From the mobile amorphous fraction and information about the crystallinity from the different methods, the rigid amorphous (interfacial) fraction (eqn. (3)) and the corresponding layer thicknesses (eqn. (4)) have been determined. Because of the very different correlation lengths of the molecular motions observed by the different methods (increasing from Raman spectroscopy, to NMR spectroscopy, to DSC), the results are expected to be different if there are broad gradients in the molecular mobility or in the structure of the different layers. If there are sharp transitions between the layers, the fractions determined by the different methods should be nearly the same. Such investigations have been made for differently crystallized PET [9, 14].

In these investigations, the crystalline fraction α from the DSC measurements was calculated by a method discussed in ref. 15. The long period L was determined from the one-dimensional electron density correlation function obtained by small-angle X-ray scattering (SAXS) [16].

The results of these calculations in comparison with X-ray diffractometry, NMR and Raman measurements at room temperature are shown in Table 1, which shows that the α, β and γ fractions obtained by the different methods in the three representative samples are consistent. Because the different methods have a different length-scale sensitivity, we conclude from this consistency that there are only weak gradients across the layers and that the transitions between the layers are relatively sharp. Thus, assumption (iii) is normally fulfilled for semi-crystalline PET. In general, the one-dimensional layer stack model described above should be useful for the description of the morphology of lamellar crystallized, semi-crystalline polymers, taking into account the rigid amorphous fraction.

Combining the long spacing L, the degree of crystallinity, e.g. from X-ray diffractometry, the mobile amorphous fraction from the glass transition (eqn. (2)), the rigid amorphous fraction from (eqn. (3)), and the layer stack model (eqn. (4)), it is possible to obtain more detailed information on the morphology of semi-crystalline polymers. For instance, Fig. 7 shows the fractions and Fig. 8 the layer thicknesses of different isothermally crystallized PET samples as a function of the crystallization temperature. For all PET samples investigated, interfacial layers of about 2 nm are obtained, independent of the crystallization conditions and the resulting morphology. The long spacing ($L = d_c + 2d_i + d_l$) and the lamellae thickness increase, and the thickness of the mobile amorphous layer also slightly increase with increasing temperature. From other crystallization regimes [8, 9], e.g. gradually or secondary crystallization, other dependences and a rather wide range of layer thicknesses were observed. Therefore, it was possible to compare parameters of the glass transition with the thickness of the mobile amorphous layer (where the glass transition takes place) [14].

The determination of the rigid amorphous fraction (β) and the

TABLE 1

Layer fractions and thicknesses for three representative PET samples determined by different methods [8, 9, 14]

	PET sample			Method
	Isothermally crystallized at 390 K	Isothermally crystallized at 450 K	Gradually crystallized at 450 K	
α	0.23	0.28	0.28	XRD
L/nm	7.3	8.6	6.9	
d_c/nm	1.7	2.4	1.9	
d_a/nm [a]	5.6 [a]	6.2 [a]	5.0 [a]	
α	0.23	0.33	0.33	DSC
β	0.53	0.43	0.48	
γ	0.24	0.24	0.19	
d_c/nm	1.7	2.8	2.2	
$2d_i$/nm	3.9	3.7	3.4	
d_i/nm	1.7	2.1	1.3	
α	–	0.28	0.29	NMR
β	–	0.45	0.45	
γ	–	0.27	0.26	
d_c/nm	–	2.4	2.0	
$2d_i$/nm	–	3.9	3.1	
d_i/nm	–	2.3	1.8	
α	0.21	0.28	0.29	Raman
β	0.44	0.41	0.44	
γ	0.35	0.31	0.27	
d_c/nm	1.5	2.4	2.0	
$2d_i$/nm	3.3	3.6	3.1	
d_i/nm	2.5	2.6	1.8	

[a] $d_a = L(1 - \alpha) = d_i + 2d_i$.

corresponding layer thicknesses (d_c, d_i, d_i) shows that the combination of the results from thermal analysis (glass transition) with those from X-ray diffractometry (α, L) yields a more detailed picture of the morphology of semi-crystalline polymers. Therefore, a better comparison between the morphology and other results is possible. But there are two problems associated with the thermal analysis of the glass transition region of semi-crystalline polymers. Firstly, there are semi-crystalline polymers, such as PE, in which the glass transition cannot be analysed. Secondly, the analysis of the glass transition leads to mean values of the layer thicknesses, (eqn. (4)), but not to their distributions. Therefore, it is necessary to find a method with which to analyse the melting region in the above-described layer stack model, including the rigid amorphous fraction.

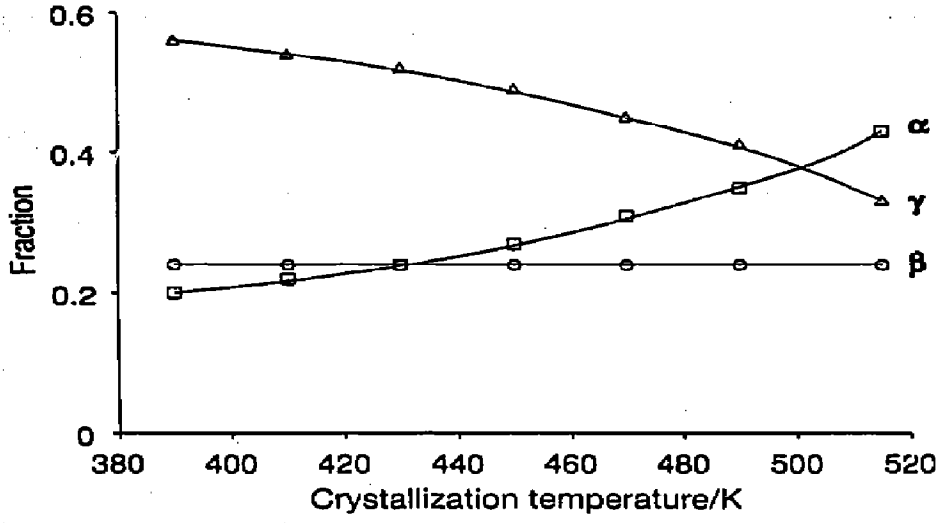

Fig. 7. Fractions of PET crystallized isothermally at different temperatures as a function of the crystallization temperature. The fractions were determined by X-ray diffractometry (α), DSC (γ), and using eqn. (3) (β).

ANALYSIS OF THE MELTING

The melting process

In lamellar crystallized polymers, there are lamellae of various thicknesses [10, 11, 17]. The melting temperatures of the lamellae are dependent on their thicknesses [18–21]. For this reason, the lamellae melt successively

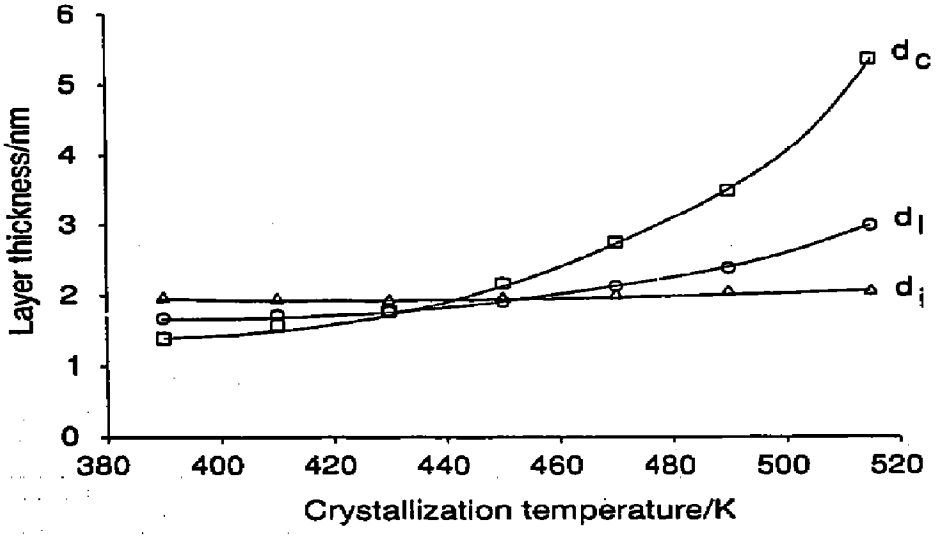

Fig. 8. Layer thicknesses of PET crystallized isothermally at different temperatures as a function of the crystallization temperature calculated by eqn. (4).

according to their thickness, if no thinning [22] or thickening of the lamellae occurs during the heating of the sample.

There are various equations that have been proposed for the melting temperature of a lamella [18–21]. Here the so-called Thomson equation, eqn. (5), is used for the description of the melting temperature of a lamella with thickness d_c

$$T_m(d_c) = T_m^0\left(1 - \frac{2\sigma_e}{\Delta h_m^0 \rho_c d_c}\right) \tag{5}$$

where T_m^0 is the equilibrium melting temperature, ρ_c the crystalline density, and σ_e the surface specific enthalpy.

The specific enthalpy diagram in Fig. 5 is for lamellae of one thickness. The specific enthalpy curve of a successively melting system is the superposition of the specific enthalpy curves of any lamellae of different thicknesses (Fig. 9). Thus, there is a broad transition region, not a sharp phase transition, in such substances. The analysis of this broad transition region should result in some additional information on the phase behaviour, i.e. on the fractions of the different states at each temperature. From this, in combination with the Thomson equation, a lamella thickness distribution can be obtained.

Method

The method used to analyse the melting process suggested here is based on the one-dimensional "three-phase" model described above. The method is iterative.

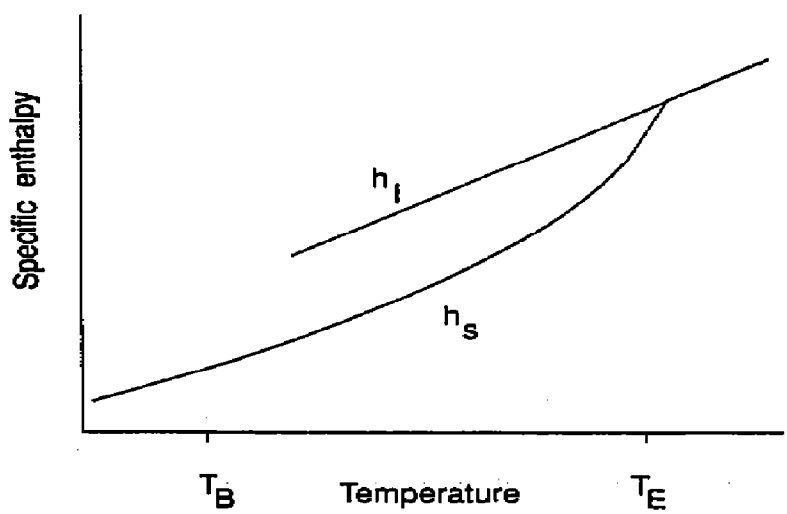

Fig. 9. Temperature dependence of the specific enthalpy in a system of lamellae of various thicknesses. T_B and T_E are the temperatures for the beginning and the end of the melting, i.e. melting of the thinnest and thickest lamellae, respectively.

The starting point of the consideration is that the heat flux Φ necessary to heat a sample linearily with time, for every temperature, can be represented by the superposition of the heat fluxes due to the baseline specific heat capacity $c_p(T)$ and the excess specific enthalpy $\Delta h_m^*(T)$, as first described in ref. 3. After normalization of the heat flux curve of the sample by dividing by the mass and the heating rate, $c_{ps}(T)$ can be expressed

$$c_{ps}(T) = c_p(T) + \frac{\mathrm{d}\,\Delta h_m^*(T)}{\mathrm{d}T} \tag{6}$$

The specific excess enthalpy $\Delta h_m^*(T)$ is the superposition of all enthalpy effects related to the melting. In a small temperature interval, this specific enthalpy can be determined from the area between the baseline c_p and the total normalized heat flux by integration.

The specific heat capacity $c_p(T)$ of the sample is the superposition of the specific heat capacities of the fractions [23]

$$c_p(T) = \gamma(T)c_{pl}(T) + (1 - \gamma(T))c_{pc}(T) \tag{7}$$

where $c_{pl}(T)$ is the specific heat capacity of the mobile amorphous fraction and $c_{pc}(T)$ represents those of the crystalline fractions, including the glassy rigid amorphous fraction. Both are available, e.g. from the ATHAS data base [24] and also for PE from ref. 25.

Consider a small temperature interval, T_1 to T_2, in the melting region of a semi-crystalline polymer. The increase of the liquid fraction ($\Delta\gamma$) within this interval is equal to the decrease in the solid fraction (crystalline, $\Delta\alpha_{1/2}$; rigid amorphous, $\Delta\beta_{1/2}$)

$$\gamma(T_2) = \gamma(T_1) + \Delta\alpha_{1/2} + \Delta\beta_{1/2} \tag{8}$$

The decrease of the crystalline fraction $\Delta\alpha_{1/2}$ in the temperature interval T_1–T_2 is determined by the specific enthalpy of fusion of infinite crystals

$$\Delta\alpha_{1/2} = \frac{\Delta h_m(T_{1/2})}{\Delta h_m^0(T_2)} \tag{9}$$

In eqn. (9), the temperature dependence of Δh_m^0 [23, 25] has to be taken into account. The heat of fusion $\Delta h_m(T_{1/2})$ alone is not directly available from a DSC trace but the superposition of all excess specific enthalpy effects related to the melting Δh_m^* is obtained. One of these additional enthalpy effects is the surface enthalpy Δh_σ of the lamellae. This enthalpy arises due to the destruction of the surfaces of the lamellae during melting and has to be taken into account. Due to the lamellae stack model, only the surfaces rectangular to the polymer chains have to be considered. With

$$\Delta h_\sigma(T_2) = \Delta\alpha_{1/2}\frac{2\sigma_e}{\rho_c d_c(T_2)} \tag{10}$$

eqn. (9) reads

$$\Delta\alpha_{1/2} = \frac{\Delta h_m^{**}(T_{1/2})}{\Delta h_m^0(T_2) - \dfrac{2\sigma_e}{\rho_c d_c(T_2)}} \tag{11}$$

where $\Delta h_m^{**} = \Delta h_m^* + \Delta h_r$ is the superposition of all other remaining enthalpy effects related to the melting. As a first approximation, we assume that there are no additional enthalpy effects. Then, Δh_m^{**} represents the heat of fusion Δh_m. A further correction will be described below.

During the melting of the lamellae in the temperature interval T_1–T_2, the hindering of the molecular mobility of the interfacial material of these lamellae disappears. Thus the interfacial fraction decreases. Because of the layer stack model (Fig. 4) this decrease is linked to the decrease in the crystalline fraction by

$$\Delta\beta_{1/2} = \frac{2d_i(T_2)}{d_c(T_2)}\Delta\alpha_{1/2} \tag{12}$$

The thickness of the lamellae $d_c(T_2)$ melting in the temperature interval considered may be obtained by the Thomson equation, eqn. (5).

From eqns. (8), (11) and (12), it follows that the fraction of the mobile amorphous material at the temperature T_2 can be expressed as

$$\gamma(T_2) = \gamma(T_1) + \left(1 + \frac{2d_i(T_2)}{d_c(T_2)}\right)\frac{\Delta h_m^{**}(T_{1/2})}{\Delta h_m^0(T_2) - \dfrac{2\sigma_e}{\rho_c d_c(T_2)}} \tag{13}$$

and with eqn. (7), a value for the specific heat capacity at T_2 is available which is necessary for the baseline.

In eqn. (13), the thickness of the interfaces of the lamellae $d_i(T_2)$, and the excess specific enthalpy Δh_m^{**} are not known, which is why an assumption is necessary to solve this equation. Therefore, it will be assumed that all interfacial layers have the same thickness, independent of the thickness of the related lamella. This assumption seems to be reasonable because the space needed for the re-entry and the loops of the polymer chains and the chain ends should not depend on the lamella thickness [26, 27]. In our investigations we start with an interface thickness of 2 nm. The estimation of the thickness will be described later.

A prerequisite for the determination of the specific enthalpy Δh_m^{**} in eqn. (13) by integration is a baseline in the temperature interval T_1–T_2, i.e. the specific baseline heat capacity c_p at T_2 has to be known (Fig. 10).

The c_p value at T_2 is not known at first. Therefore, the value at T_1 is taken for the first approximation (Fig. 10). A corrected value for the

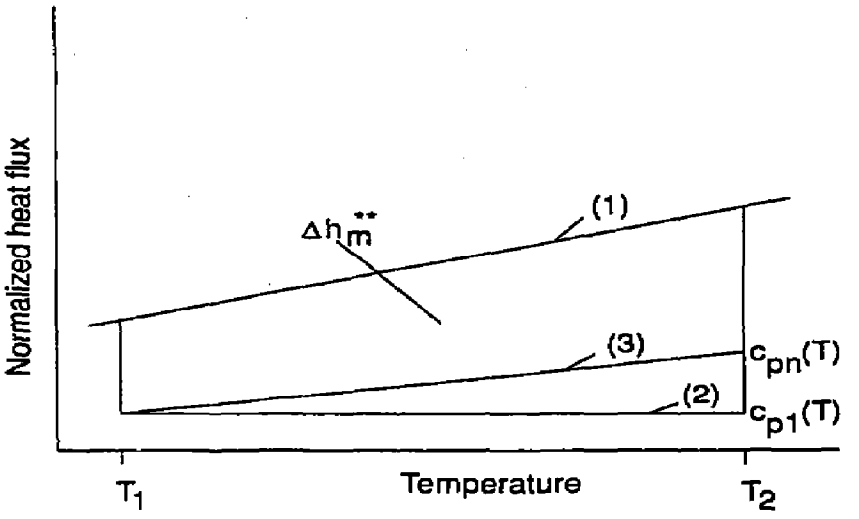

Fig. 10. Determination of the excess specific enthalpy Δh_m^{**} from the normalized heat flux (1) in a small temperature interval from T_1 to T_2: $c_{p,1}(T_2)$, first used value for the baseline c_p at T_2; $c_{p,n}(T_2)$, iteratively calculated value; (2) and (3) are the baselines in the temperature interval, arbitrarily chosen and iteratively calculated, respectively.

specific baseline heat capacity at T_2 is then obtained from eqns. (13) and (7). This calculation has to be repeated until the value for the specific baseline heat capacity at T_2 does not change more than 0.1%. In this way it is possible to estimate the decrease in the crystalline and rigid amorphous fractions as well as the increase in the mobile amorphous fraction.

By shifting the temperature interval T_1-T_2 over the normalized heat flux curve, the melting process of the investigated sample may be analysed. For this analysis, two conditions have to be met.

(i) The liquid amorphous fraction has to be known at the first investigated temperature T_{1i}. From eqn. (6), it follows that at a temperature where no melting occurs, the specific baseline heat capacity can be calculated from the heat flux. Then the mobile amorphous fraction at this temperature $\gamma(T_{1i})$ can be calculated by eqn. (7). The measurements have to be started at this temperature.

(ii) At the last investigated temperature T_{1e}, all the crystalline material has to be in a molten state ($\alpha = \beta = 0$; $\gamma = 1$).

The first condition may be fulfilled just above the glass transition region, because normally no melting occurs there [28]. Condition (ii) should be fulfilled at temperatures above the equilibrium melting temperature of the polymer under investigation.

At the end of the first run (calculation with $d_i = 2$ nm) at the temperature T_{1e}, above the equilibrium melting temperature, the result $\alpha \neq 0$, $\beta \neq 0$, and $\gamma \neq 1$ is obtained; this does not happen in reality because the thickness of the interfaces d_i in eqn. (13) is needed but not known.

Thus, the thickness of the interface layers d_i is changed and the calculation is re-started at a temperature just above the glass transition T_g. This is repeated until $\alpha = 0$, $\beta = 0$ and $\gamma = 1$ is reached at T_E.

After this double iteration, the temperature dependence of the liquid amorphous fraction $\gamma(T)$, the specific baseline heat capacity of the sample $c_p(T)$, and the interfacial thickness d_i are known. Moreover, the change in the crystalline material in each temperature interval $\Delta\alpha(T_{1/2})$ is obtained from the calculation. From this, the crystalline fraction for every temperature T follows

$$\alpha(T) = \sum_{x=T}^{T_E} \Delta\alpha(x) \tag{14}$$

and the interfacial fraction $\beta(T)$ can be obtained from eqn. (3).

Correction of the method in the case of supercooling [a]

A prediction of the above-described method is that only the heat of fusion and the surface enthalpy of the lamellae are related to the excess enthalpy. In the case of substances with a difference between the crystallization and the melting temperature of the lamellae of the same thickness, an additional enthalpy effect related to the interfacial fraction occurs. This enthalpy effect and the corresponding completion of the method are described here.

The molecular mobility of the material in the interfaces of the lamellae is hindered by the lamellae (see above). This hindering of the molecular mobility appears at the crystallization temperature T_c of each lamellae. The material of the interfaces will become rigid there. Therefore, the slope of the specific enthalpy function of the interfaces of the lamellae changes from that of the liquid to that of the solid state (Fig. 11).

During the subsequent heating the lamellae will melt at the temperature T_m. The hindering of the molecular mobility of the interfaces of these lamellae will disappear at this temperature. Therefore, the specific enthalpy function of the interfaces of the lamellae will reach that of the liquid amorphous state. If the melting temperature is significantly higher than that of crystallization, the "glass transition" of the interfaces will be combined with a jump in the specific enthalpy (Fig. 11), which is the same effect as in the case of enthalpy relaxation in amorphous polymers after annealing below T_g or after cooling at cooling rates lower than the heating

[a] The idea for this correction was given to the authors by J. van Ruiten (DSM, Geleen). See also ref. 40.

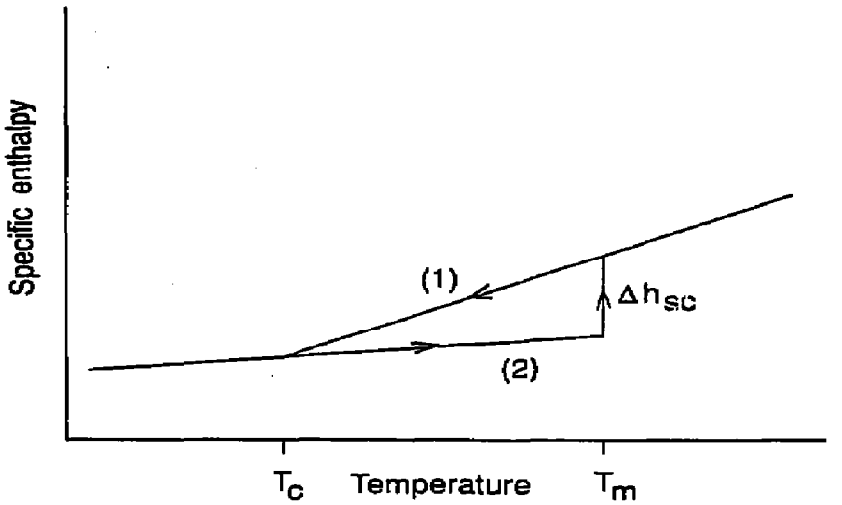

Fig. 11. Temperature dependence of the specific enthalpy of the interfaces. (1), cooling curve with crystallization at T_c; (2), heating curve with melting at T_m; Δh_{sc}, specific enthalpy due to the difference between the crystallization and melting temperature.

rate used. The specific enthalpy of this jump is related to the melting and has therefore to be taken into account.

Because the slope (specific heat capacity) of the crystalline fraction is equal to the slope of curve (2) (rigid amorphous) in Fig. 11, Δh_{sc} depends on the change of the difference between $h_l(T)$ (curve (1)) and $h_c(T)$ in the interval T_c–T_m (supercooling ΔT_{sc}). Moreover, Δh_{sc} depends on the change of the rigid amorphous fraction $\Delta\beta_{1/2}$ in the temperature interval T_1–T_2. This can be written as (see Fig. 5)

$$\Delta h_{sc}(T_m) = (\Delta h_m^0(T_m) - \Delta h_m^0(T_c))\,\Delta\beta_{1/2} \tag{15}$$

To obtain the heat of fusion, the excess specific enthalpy Δh_m^{**} in eqn. (13) has to be reduced by this specific enthalpy Δh_{sc}. If the supercooling of the lamellae melting at T_2 is ΔT_{sc}, the second factor in eqn. (13), which is the change in the crystalline fraction $\Delta\alpha_{1/2}$ (compare eqns. (11) and (13)), reads

$$\Delta\alpha_{1/2} = \frac{\Delta h_m^{**}(T_{1/2}) - \Delta\beta_{1/2}[\Delta h_m^0(T_2) - \Delta h_m^0(T_2 - \Delta T_{sc})]}{\Delta h_m^0(T_2) - \dfrac{2\sigma}{\rho_c d_c(T_2)}} \tag{16}$$

with $\Delta T_{sc} = T_m - T_c$ ($\approx$12 K for PE [3]). Because $\Delta\beta_{1/2}$ is dependent on $\Delta\alpha_{1/2}$ (eqn. (12)), and is not known at first, an additional iteration is necessary until $\Delta\alpha_{1/2}$ is constant.

The enthalpy effect related to the supercooling results in a relatively small correction (less than 1%) in the fractions of PE at low temperatures (melting of thin lamellae) and can be neglected.

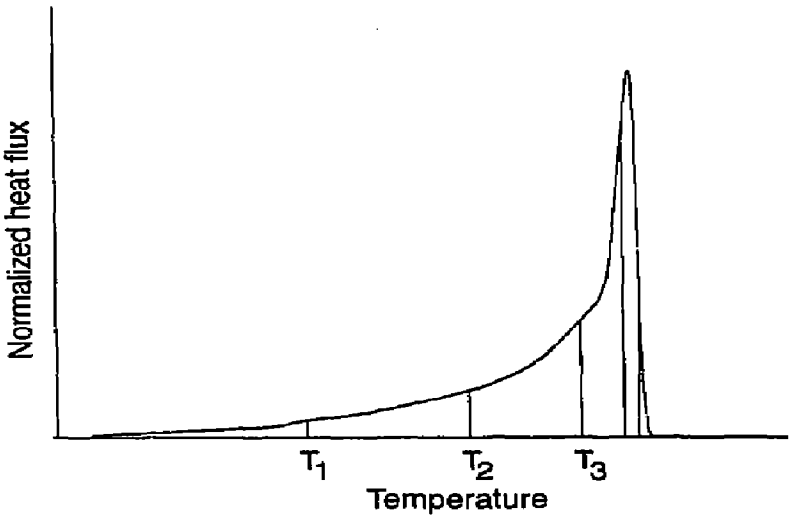

Fig. 12. Graduation (schematic) of the temperature axis in intervals of the same range of the lamella thickness, calculated using the Thomson equation.

Determination of the lamellae thickness distribution

The crystalline fraction of a polymer may be considered as a system of many components in which all components contain all lamellae of the same thickness [29]. All lamellae of the same thickness will melt at the same temperature (eqn. (5)). Thus, it should be possible to estimate the lamellae thickness distribution from the normalized heat flux curves. If no recrystallization occurs, the fraction of lamellae melting in a temperature interval can be determined from the heat of fusion in this interval [30, 31]. The estimation of the lamellae thickness distribution will now be described.

To determine the lamellae thickness distribution, it is necessary to divide the melting region into temperature intervals ($T_{i-1} \cdots T_i$) which represent equal ranges in the lamellae thickness (Fig. 12). Because the melting temperature of a lamella of thickness d_c is given by the Thomson equation, eqn. (5) ($T_m \propto 1/d_c$), the temperature intervals are not equidistant.

The heat necessary to melt N_i lamellae within the temperature interval $T_{i-1}-T_i$ ($\Delta h_m(T_{i-1/i})$) is proportional to the total crystalline volume V_i melting in the temperature interval considered

$$\Delta h_m(T_{i-1/i}) = \frac{\Delta h_m^0(T_i)\rho_c}{m} V_i \tag{17}$$

where m is the sample mass.

Because V_i represents the volume of the lamellae melting in that range of lamellae thickness limited by the thicknesses corresponding to T_{i-1} and T_i,

it is possible to calculate the volume fraction $\Phi_V(d_{c_i})$ of the lamellae thickness distribution by

$$\Phi_V(d_{c_i}) = \frac{V_i}{\sum_n V_n} = \frac{\frac{\Delta h_m(T_{i-1/i})}{\Delta h_m^0(T_i)} \frac{m}{\rho_c}}{\sum_n V_n} = \frac{\Delta\alpha(T_{i-1/i}) \frac{m}{\rho_c}}{\sum_n V_n} \tag{18}$$

In addition to the lamellae thickness distribution, the specific inner surface O_s (the surface perpendicular to the chain direction of the lamellae) may also be calculated from geometrical considerations

$$\frac{O_s}{m} = \frac{2}{\rho_c} \sum_i \frac{\Delta\alpha(T_{i-1/i})}{d_{c_i}} \tag{19}$$

For some investigations, e.g. comparison with electron microscopy results [10, 11], the calculation of a number distribution, rather than a volume (or mass) distribution is desirable. But the calculation of such a distribution is only possible if the area of each lamellae is known.

Results

The measurements were performed with a computer-controlled, well stabilized Perkin-Elmer DSC-2 [32, 33]. All measurements contain isothermal portions at the beginning and end of the scan. An empty pan measurement was subtracted and a sapphire correction was performed in order to obtain the sample heat flux. The scan rate was 10 K min^{-1} and the sample mass was about 5 mg (thin foil) in order to reduce smearing due to the heat transfer. A sample mass of about 5 mg is necessary because of the precision of the specific heat capacity determination at T_i, necessary to get an accurate value for the mobile amorphous fraction at this temperature eqn. (7).

The measurements presented here were carried out to answer two questions. Firstly, the results obtained with the "three-phase" model were compared with those of the "two-phase" model (total enthalpy method) to obtain information on the effect of the interfaces of the lamellae on the results of the melting analysis. Secondly, the results of the DSC measurements were compared with those of SAXS measurements in order to evaluate the DSC results.

To demonstrate the capability of the suggested method, results obtained from a low-density polyethylene, Lupolen LDPE 1840 D, and a high-density polyethylene, Lupolen HDPE 6011 L, from BASF AG, are presented. PE was used as an example in which the possible existence of rigid amorphous material inside a semi-crystalline sample and of interfaces

TABLE 2
Parameters for poly(ethylene) (PE) used for the evaluation of the DSC measurements

Parameter	Value	Parameter	Value
T_m^∞	415 ± 0.5 K [34, 35]	ΔT_w	12 ± 1 K [3]
Δh_m^∞	293 ± 0.2 J g^{-1} [25, 36]	T_0	230 K
σ_e	0.0795 ± 0.0025 J m^{-2} [31, 37]	T_0	414.9 K
$\rho_c(T_m^\infty)$	0.952 g cm^{-3} [38, 39]		

in the crystalline lamellae are ignored. In our approach, it is postulated that there is material which is in neither the crystalline nor the liquid amorphous states.

The parameters used in the DSC investigations are shown in Table 2. The specific heat capacities of the crystalline and the liquid amorphous fractions are taken from ref. 25. The quality of these heat capacities, as well as the measured value, determines the quality of the calculations. Because the specific heat capacities in ref. 25 are calculated on the basis of a two-phase approach and because there are some questions concerning the increase in the difference between $c_{pa}(T)$ and $c_{pc}(T)$ between 120 and 290 K [25], it may be useful to re-examine the data using a "three-phase" approach. In this paper, we present a way of describing the melting of polymers from the calorimetric investigations. Therefore, we take the c_p data from ref. 25 as a first and, in our opinion, a good approximation.

Figures 13 and 14 show the calculated c_p baselines for the determination of the excess specific enthalpy and the measured normalized heat flux of the LDPE and the HDPE. According to the total enthalpy method, the baseline was recalculated from $\alpha(T)$ with eqn. (7) and $\gamma(T) = 1 - \alpha(T)$.

The temperature dependence of the fractions is shown for LDPE in Fig. 15 and for HDPE in Fig. 16. From this, in combination with other methods, e.g. X-ray diffractometry, a more detailed description of the morphology at every temperature is available.

To compare the results obtained by the "two-" and the "three-phase" models, the LDPE and HDPE samples were examined. The results of the "two-phase" model were derived by the total enthalpy method proposed by Gray [1]. The temperature dependence of the crystalline fraction calculated in this way is also shown in Figs. 15 and 16 (dotted line).

It may be seen from Figs. 15 and 16 that the crystallinities obtained from both methods are nearly the same in the main melting region (350–415 K). At lower temperatures, there are deviations between the results of the two methods. The crystallinities calculated by the "three-phase" model at 250 K are about 0.03 (for HDPE 6011 L) and 0.05 (for LDPE 1840 D), higher than those obtained by the total enthalpy method. At room temperature, this deviation is nearly half of those observed at 250 K.

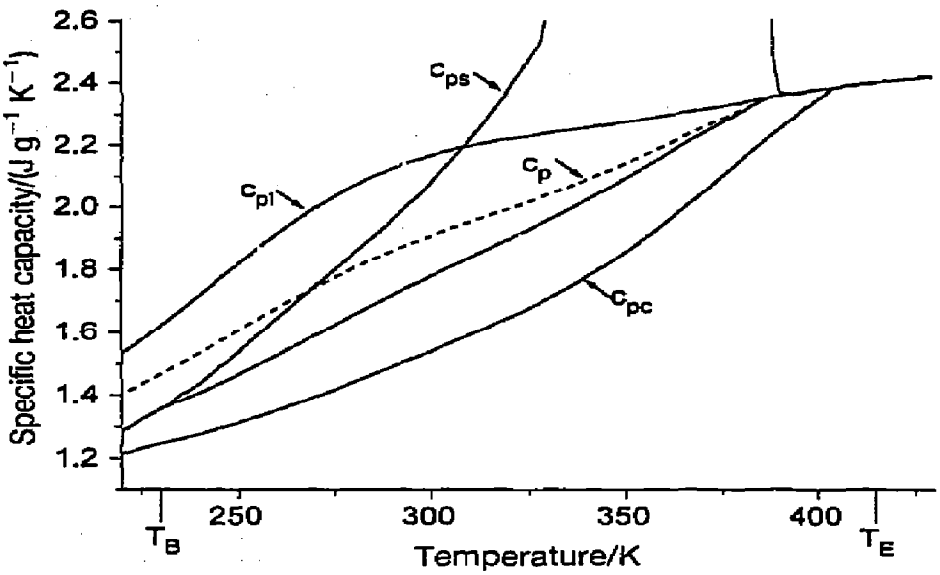

Fig. 13. Normalized heat flux of the semi-crystalline sample ($c_{p,s}$), the reference specific heat capacities ($c_{p,l}$, $c_{p,c}$), and the calculated baseline (c_p) of LDPE 1840 D. The c_p baselines are calculated according to the total enthalpy method (– – –) and the "three-phase" model (—).

The crystallinity calculated using the "three-phase" model is nearly constant (for HDPE 6011 L) or shows a slightly decrease (up to room temperature for LDPE 1840 D). In contrast to this, there is a small but unrealistic increase in the crystallinities calculated by the total enthalpy method in this region, as also reported by Mathot and van Ruiten [40]. This

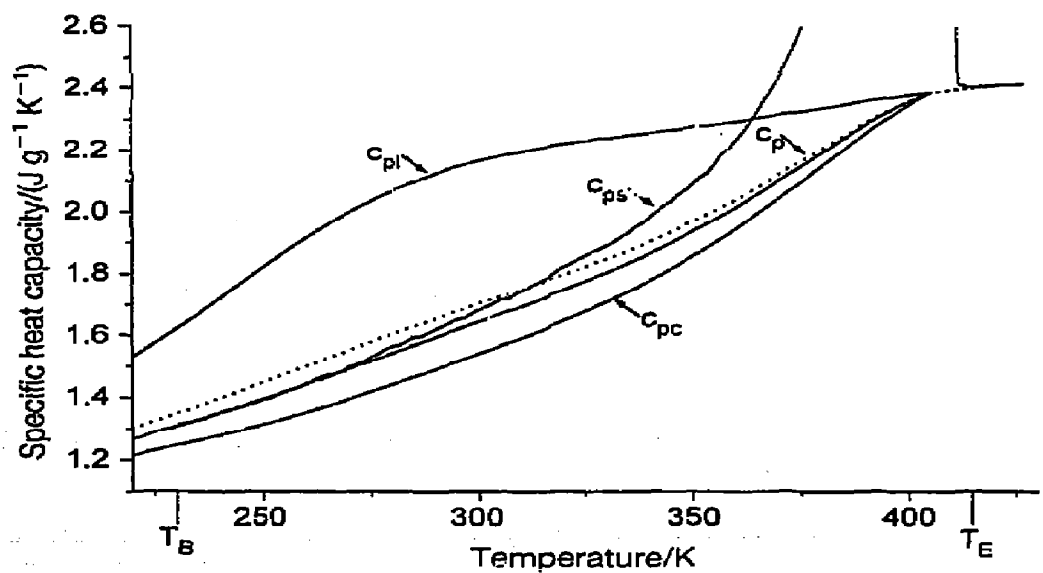

Fig. 14. Normalized heat flux of the semi-crystalline sample ($c_{p,s}$), the reference specific heat capacities ($c_{p,l}$, $c_{p,c}$), and the calculated baseline (c_p) of HDPE 6011 L. The c_p baselines are calculated according to the total enthalpy method (· · ·) and the "three-phase" model (—).

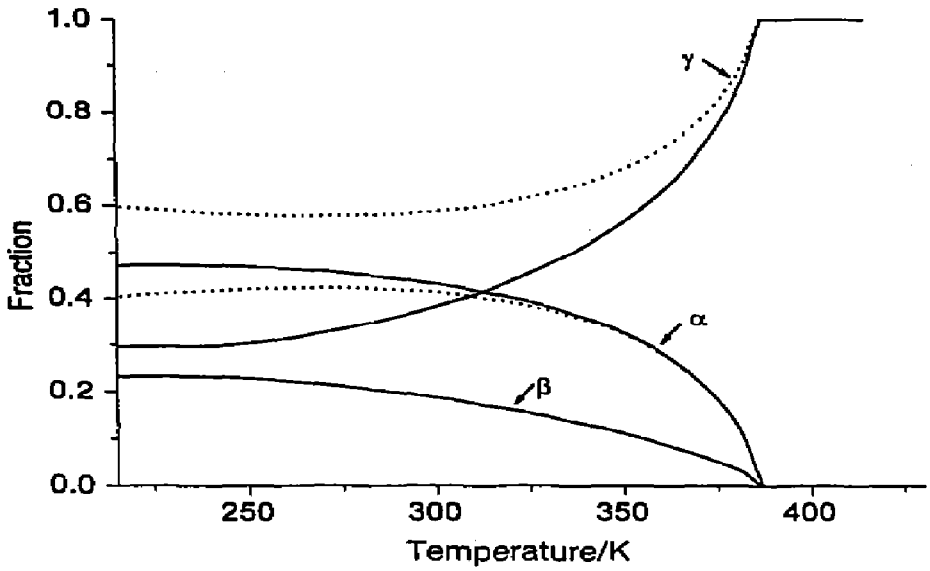

Fig. 15. Temperature dependence of the fractions of LDPE 1840 D. Crystallinities determined by the total enthalpy method (· · ·) and by the method based on the "three-phase" model (—).

is also apparent in the lamellae thickness distributions. In the lamella stack model, the reason for the increase in the crystallinity at low temperature is the formation of very thin lamellae. This is why the lamellae thickness distributions derived by the total enthalpy method begin with negative

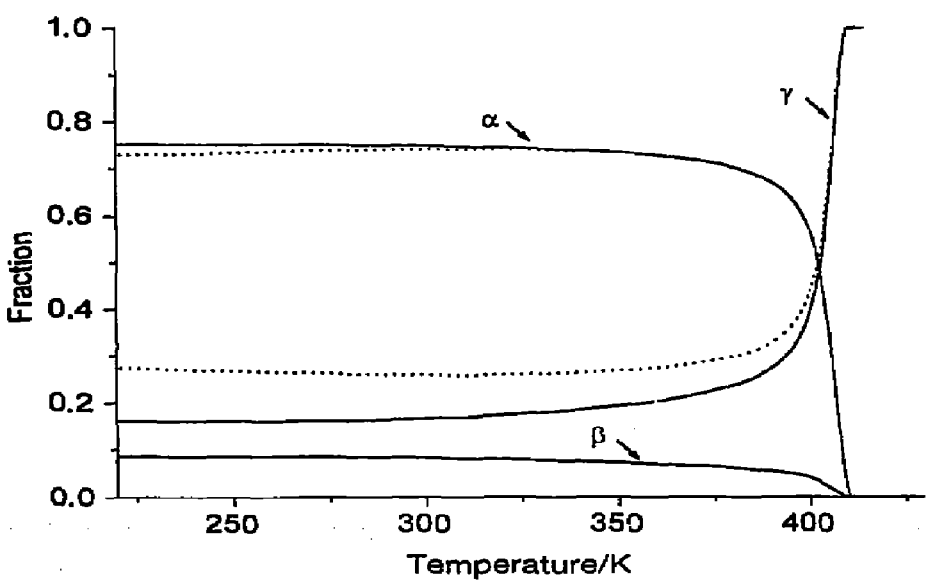

Fig. 16. Temperature dependence of the fractions of HDPE 6011 D. Crystallinities determined by the total enthalpy method (· · ·) and by the method based on the "three-phase" model (—).

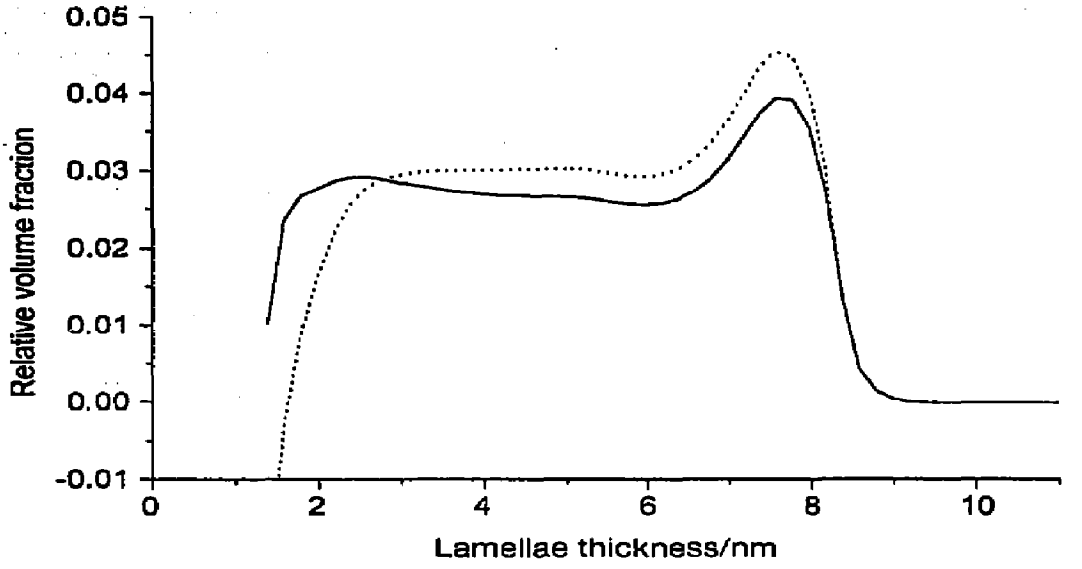

Fig. 17. Lamellae thickness distribution of LDPE 1840 D determined on the basis of the two-phase (· · ·) and "three-phase" (—) models.

values. Therefore, the lamellae thickness distribution obtained from the "three-phase" model results in higher values at low lamellae thicknesses (Figs. 17, 18). The specific inner surface O_s, the mean value of the lamellae thicknesses distribution $\overline{d_c}$, and the interfacial thickness d_i at 230 K were obtained from the "three-phase" model (for LDPE, $O_s = 600\ m^2\ g^{-1}$, $\overline{d_c} = 5$ nm, $d_i = 1$ nm; for HDPE, $O_s = 100\ m^2\ g^{-1}$, $\overline{d_c} = 23$ nm, $d_i = 0.9$ nm).

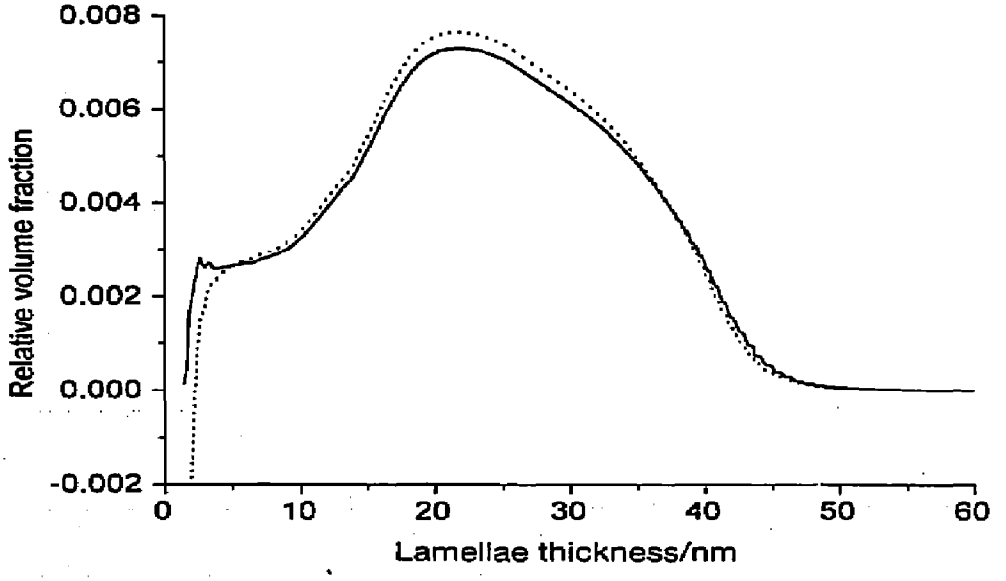

Fig. 18. Lamellae thickness distribution of HDPE 6011 L determined on the basis of the two-phase (· · ·) and "three-phase" (—) models.

Because in our model (constant interfacial layer thickness for all lamellae) the proportion of the interfacial fraction increases with decreasing lamellae thickness, the rigid amorphous fraction particularily influences the results connected with the melting of thin lamellae (Figs. 13–18). The first results from the "three-phase" model presented here are influenced by different factors. In general, the accuracy of the c_p measurements at T_B determines the value of the mobile fraction at this temperature and therefore the results of the whole calculation. The second uncertainty is due to the parameters used for the calculation (Table 2), including the reference $c_p(T)$ for the liquid and the crystalline fractions.

The correlation between the morphological parameters obtained by DSC on the basis of the "three-phase" layer stack model and the results from other methods shows that this model is applicable in the investigation of polymers. The advantage of the DSC method is its low expense (low sample mass, short time for measurements). But it may be considered as only an addition to the methods for morphological investigations because, for example, the thickness of the amorphous layers and the long period cannot be deduced using this technique.

CONCLUSIONS

Thermal analysis can provide information on the morphology of semi-crystalline polymers from an analysis of the melting process and, in addition, from the glass transition. The comparison of this information obtained on the basis of a two-phase model shows that there are deviations from the model. Wunderlich and coworkers [4, 5] have shown that this can be explained by the presence of rigid amorphous material in the sample. Therefore, it seems necessary to analyse the glass transition and the melting process with regard to this material. A way of analysing the melting on the basis of a one-dimensional layer stack model, in which the rigid amorphous material is attributed to the interfaces of the crystalline lamellae, is suggested here. To achieve a solution to this problem, it is necessary to make an assumption regarding the relation between the interfacial layer thickness and the thickness of the lamellae.

Here it is assumed that the thickness of the interfacial layer is constant, i.e. it is independent of the lamellae thickness. The iterative method supplies the temperature dependence of the crystalline, liquid amorphous, and interfacial fractions, as well as the thickness of the interface. In addition, the temperature dependence of the specific heat capacity (without excess contributions) of the sample is available. In a second step, the lamellae thickness distribution, the mean lamella thickness, and the specific inner surface may be determined.

Because it is necessary to calculate the mobile amorphous fraction at the starting temperature from the measured specific heat capacity at this

temperature, the error in the fraction corresponds to the error in the determination of the specific heat capacity. For a power-compensated DSC, this uncertainty is in the order of 1%. Therefore, this method of analysing the melting, taking into account the rigid amorphous fraction, requires that the c_p measurements are very accurate. In Fig. 13 (LDPE), it can be seen that near $T_u = 230$ K, condition (i) (above) may not be fulfilled: compare the $c_{p,s}$ and c_p values from the "three-phase" model in this range with those of Fig. 14.

The results of the analyses of HDPE and LDPE samples were compared with those obtained on the basis of a two-phase model. This comparison shows deviations in the low temperature region which are connected with the melting of thin lamellae. The two-phase model gives an unrealistic increase in the crystallinity from 250 K up to room temperature. Therefore, the results obtained on the basis of the "three-phase" model seem to be more correct. A comparison of these results with those of X-ray investigations shows a good correlation. Therefore, it may be concluded that the method proposed here provides a good addition to other methods of morphological investigations and that the assumption that the interfacial layer has a constant thickness independent of the lamellae thickness, is not totally wrong.

ACKNOWLEDGEMENTS

The authors thank G.W.H. Höhne (Ulm), V.B.F. Mathot and J. van Ruiten (DSM, Geleen), M.J. Richardson (National Physical Laboratory, Teddington) and F. Fabry (Rostock) for helpful discussions, and the Deutsche Forschungsgemeinschaft; SFB 239 for financial support.

REFERENCES

1 A.G. Gray, Thermochim. Acta, 1 (1970) 563.
2 M.J. Richardson, in G. Allen (Ed.), Comprehensive Polymer Science Vol. A: Polymer Characterisation, Pergamon Press, 1989, p. 886.
3 V.B.F. Mathot and M.F.J. Pijpers, Thermochim. Acta, 151 (1989) 241.
4 H. Suzuki, J. Grebowicz and B. Wunderlich, Brit. Polym. J., 17 (1986) 1.
5 S.Z.D. Cheng, M.-Y. Cao and B. Wunderlich, Macromolecules, 19 (1986) 1868.
6 H. Dehne, A. Roger, D. Demus, S. Diele, H. Kresse, G. Pelzl, W. Wedler and W. Weissflog, Liquid Crystals, 6 (1989) 47.
7 C. Schick, B. Stoll, J. Schawe, A. Roger and M. Gnoth, Progr. Colloid Polym. Sci., 85 (1991) 148.
8 C. Schick, Thesis B, PH Güstrow, 1988.
9 C. Schick, F. Fabry, U. Schnell, G. Stoll, L. Deutschbein and W. Mischok, Acta. Polym., 39 (1988) 705.
10 I.G. Voigt-Martin, G. M. Stack, A.J. Peacock and L. Mandelkern, J. Polym. Sci. Part B. Polym. Phys., 27 (1989) 957.
11 G. Michler, H. Steinbach and K. Hoffmann, Acta Polym., 34 (1983) 533.

12 G.C. Claver, R.L. Buchdahl and J. Miller, J. Polym. Sci., 20 (1956) 202.
13 C. Schick, L. Krämer and W. Mischok, Acta Polym., 36 (1985) 47.
14 C. Schick and E. Donth, Phys. Scri., 43 (1991) 423.
15 C. Schick and J. Gnoza, Acta Polym., 36 (1985) 181.
16 F. Fabry, Thesis B, PH Güstrow 1990.
17 I.G. Voigt-Martin and L. Mandelkern, J. Polym. Sci. Part B Polym. Phys., 27 (1989) 967.
18 F. Meißner, Z. Allg. Chem., 110 (1920) 169.
19 P.J. Flory, Principles of Polymer Chemistry, Cornell University Press, Ithaca, N.Y., 1953, p. 563.
20 L. Mandelkern, J.M. Price, M. Gopalan and J.G. Fatou, J. Polym. Sci. Part A-2, 4 (1966) 385.
21 H.G. Kilian, Kolloid Z. Z. Polym., 202 (1965) 97.
22 G.R. Strobl, T. Engelke, T. Maderek and G. Urban, Polymer, 24 (1983) 1585.
23 U. Gaur and B. Wunderlich, J. Phys. Chem. Ref. Data, 10 (1981) 119.
24 ATHAS Advanced Thermal Analysis.
25 V.B.F. Mathot, Polymer, 25 (1984) 579. Errata: Polymer, 27 (1986) 969.
26 W.D. Varnell, J.R. Harrison and S.J. Kozminski, J. Polym. Sci. Part B Polym. Phys., 19 (1981) 1237.
27 D.M. Sadler and R. Harris, J. Polym. Sci., Part B, Polym. Phys., 20 (1982) 561.
28 B. Wunderlich, Polymer, 27 (1986) 575.
29 W. Glenz, H.G. Kilian, D. Klattenhoff and F. Stracke, Polymer, 18 (1977) 685.
30 A. Wlochowicz and M. Eder, Polymer, 25 (1984) 1268.
31 H.-J. Dalcolmo, Theses, TH Merseburg, 1989.
32 M. Alsleben, Theses, Rostock, 1992.
33 W. Winter and G.W.H. Höhne, Thermochim. Acta, 187 (1991) 257.
34 M.G. Broadhurst, J. Res. Natl. Bur. Stand. Sect. A, Physics and Chemistry, 3 (1962) 241.
35 B. Wunderlich and G. Czornyj, Macromolecules, 10 (1977) 906.
36 B. Wunderlich and H. Baur, Adv. Polym. Sci., 7 (1970) 151.
37 K.H. Illers and H. Hendus, Macromol. Chem., 113 (1968) 1.
38 P.R. Swan, J. Polym. Sci., 56 (1962) 403.
39 S. Matsuoka, J. Polym. Sci., 57 (1962) 569.
40 V.B.F. Mathot and J. van Ruiten, Thermal Characterization of States of Matter, in V.B.F. Mathot (Ed.), Calorimetry and Thermal Analysis of Polymers, Hanser Publishers, 1994.